Pergamon

Int. J. Solids Structures Vol. 33, No. 14, pp. 2055–2074, 1996
Copyright © 1996 Published by Elsevier Science Ltd
Printed in Great Britain. All rights reserved
0020–7683/96 $15.00 + .00

0020–7683(95)00145–X

A SIMPLIFIED ANALYSIS OF RECTANGULAR CELLULAR PLATES

HIDEO TAKABATAKE
Department of Architecture, Kanazawa Institute of Technology, Ohogigaoka 7-1, Nonoichi-machi, Ishikawa-gun, Ishikawa, 921 Japan

NOBUFUSA YANAGISAWA
Structural Engineering Section, Research Institute, Nihon-Kokudo-Kaihatsu Corporation, Kanagawa, 243-03, Japan

and

TAKASHI KAWANO
Structural Engineering Section, Department of Building Design, Takenaka Corporation, Osaka, 541, Japan

(*Received* 14 *November* 1994; *in revised form* 21 *June* 1995)

Abstract—This paper presents a general analytical method for rectangular cellular plates with arbitrarily-positioned large voids, in which the bending and the transverse shear deformations along with the frame deformation are considered. The frame deformation is defined as the flexural deformation of frame composed of the top and bottom platelets and of partitions in the cellular plate. The discontinuous variation of the bending and transverse shear stiffnesses due to the voids is expressed continuously by the use of a specific function, defined to exist continuously in a prescribed region. The bending stiffness is given by the actual bending stiffness at each point. The transverse shear stiffness per void is given by an equivalent transverse shear stiffness, which is calculated from the stiffness of a frame and partitions, like shear walls surrounding each void, and depends on the shape of each void. The governing equations are formulated by means of Hamilton's principle. Neglecting the effect of voids, the proposed governing equations reduce to the Mindlin theory. Static and dynamic solutions are obtained by the Galerkin method. The approximate solution for dynamic plates is proposed. The numerical results obtained from the proposed theory for simply-supported and clamped cellular plates show good agreement with results obtained from the finite element method. The theory proposed here includes the Mindlin and Reissner theories, and Takabatake's theory [Takabatake, H. (1991). Static analyses of elastic plates with voids. *Int. J. Solids Structures* **28,** 179–196] based on the Kirchhoff-Love hypothesis.

1. INTRODUCTION

Recently, cellular plates have been used as building slabs. The deformation is characterized by the frame deformation, as shown in Fig. 1. This is the flexural deformation of a frame,

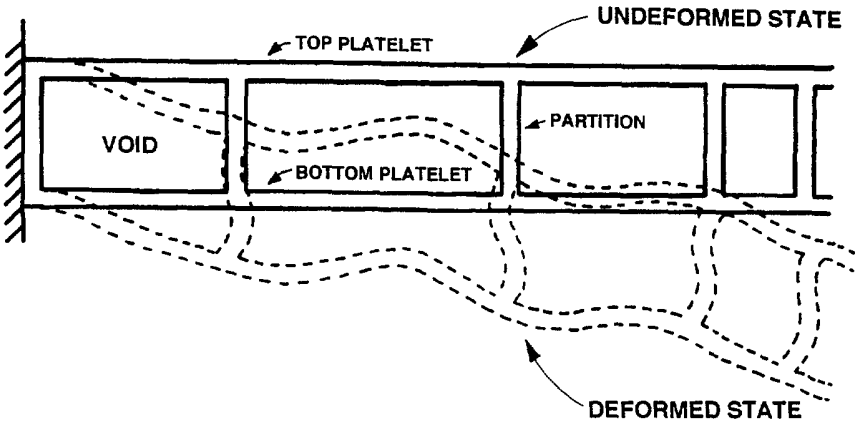

Fig. 1. Frame deformation of cellular plate.

composed of top and bottom platelets and of partitions surrounding a void. Most methods for the analysis of cellular plates are based on an equivalent plate analogy. A number of authors have proposed rigidity coefficients, for example, Crisfield and Twemlow (1971), Cope *et al.* (1973), Holmberg (1960), Sawko and Cope (1969), and Elliott (1978). However, the above equivalent approaches cannot apply to a plate with irregularly-spaced voids and/or with voids of different cross-sections, because the stiffness depends on the size and position of voids used.

On the other hand, although the finite element method is effective for a cellular plate, it needs a computer of great capacity and is both costly and time-consuming for computation. So, in the preliminary stage of design, the use of the finite element method is not practical. Takabatake (1991a, 1991b) presented a general and simplified analytical method for static and dynamic analysis of plates with arbitrarily-positioned voids. The discontinuous variation of stiffness of such a plate was expressed as a continuous function by means of a specific function based on Dirac function. Since this theory is based on the validity of the Kirchhoff-Love hypothesis, it cannot apply to a cellular plate, because the deformation is dominated by the frame deformation.

Reissner (1945) and Mindlin (1951) presented theories including the transverse shear deformation for a rectangular solid plate, in which the bending rigidity and transverse shear stiffness are constant. However, since a cellular plate with arbitrarily-positioned and arbitrarily-opening voids is dominated by the frame deformation. the bending and transverse shear stiffnesses vary discontinuously. So, it is desired, for practical use, to formulate a general and simplified analytical method for such a cellular plate.

The purpose of this paper is to propose a general and simplified method for a rectangular cellular plate with arbitrarily-positioned voids, in which bending and the transverse shear deformation, along with the frame deformation, are considered. The discontinuous variation of the bending and transverse shear stiffnesses is treated as a continuous function by means of a specific function proposed by Takabatake (1988, 1991a, 1991b). This treatment is independent of the previous equivalent plate analogy for rectangular plates.

First, the general governing equations for a rectangular cellular plate with the transverse shear deformation along with the frame deformation are proposed by using Hamilton's principle. Second, the static solutions are presented by the use of the Galerkin method. Third, the natural frequencies are presented by means of the Galerkin method; and an approximate expression for the natural frequency is proposed. Fourth, the forced vibrations are presented by the use of the linear acceleration method. For practical use, the approximate solutions are proposed for general external loads. The exactness of the theory and approximate solutions proposed here are established from numerical results by comparing the results obtained from the proposed theory for simply-supported and clamped cellular plates with the results obtained from FEM code NASTRAN.

2. GOVERNING EQUATIONS OF A CELLULAR PLATE WITH TRANSVERSE SHEAR DEFORMATIONS ALONG WITH FRAME DEFORMATION

Consider a rectangular cellular plate with arbitrarily-positioned voids. A Cartesian coordinate system x, y, z is employed. Assume that each void is a rectangular parallelepiped whose ridgelines are parallel to the x- or y-axis and which is symmetrically positioned with respect to the middle plane of the cellular plate, as shown in Fig. 2. The midpoint, widths, and height of the i, jth void are indicated by (x_i, y_j), $b_{xi,j}$, $b_{yi,j}$, and $h_{i,j}$, respectively. The size and position of each void are arbitrary except for the mentioned assumption.

This paper considers the bending of an isotropic cellular plate subject to small deformations, including the transverse shear deformation along with the frame deformation. The deformation of cellular plates is assumed to be adequately defined by describing the geometry of its middle surface, which is a surface that bisects the plate thickness, h_0, at each point. Then, neglecting the effect of shear-lag and considering the in-plane mean transverse deformation, the displacement components, $\bar{U}$, $\bar{V}$, and $\bar{W}$ on a general point of the cellular plate are given as

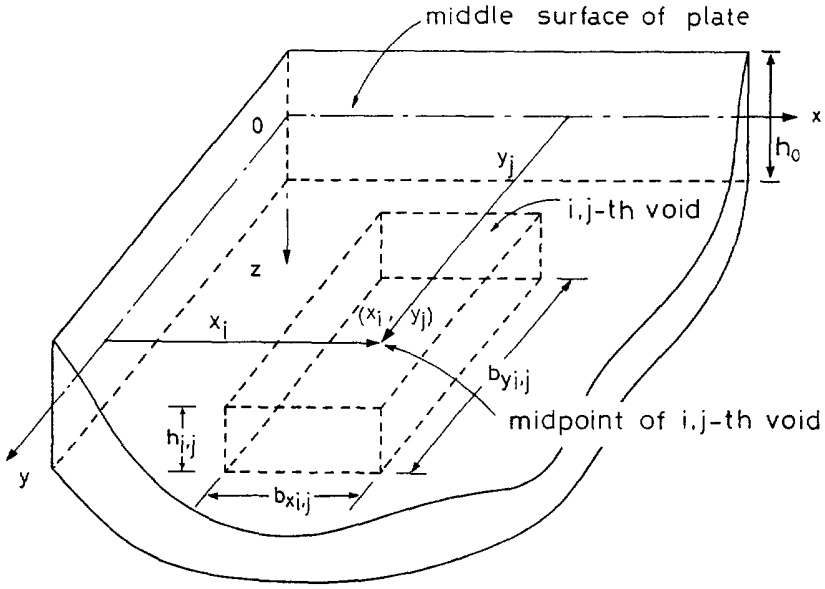

Fig. 2. Details of void.

$$\bar{U}(x, y, z, t) = z\theta_x(x, y, t) \tag{1}$$

$$\bar{V}(x, y, z, t) = z\theta_y(x, y, t) \tag{2}$$

$$\bar{W}(x, y, z, t) = w(x, y, t) \tag{3}$$

in which $w(x, y, t)$ = the lateral displacement on the middle surface; and θ_x and θ_y = the rotational angles about y- and x-axes, respectively; and z = the distance measured from the middle surface of the plate. These displacement and rotational angles are considered positive when they point toward the positive direction of the z-coordinate axis and clockwise with respect to the y- and x-coordinate axes, respectively.

The strain energy U for the current problem is given by

$$U = \frac{1}{2}\iint [M_x\theta_{x,x} + M_y\theta_{y,y} + M_{xy}(\theta_{x,y} + \theta_{y,x}) + Q_x(w_{,x} + \theta_x) + Q_y(w_{,y} + \theta_y)]\,\mathrm{d}x\,\mathrm{d}y \tag{4}$$

in which M_x, M_y, and M_{xy} = the bending and twisting moments per unit width, respectively; Q_x and Q_y = the transverse shear forces per unit width. The bending and twisting moments are given by

$$M_x = D_0\,\mathrm{d}(x, y)(\theta_{x,x} + \nu\theta_{y,y}) \tag{5}$$

$$M_y = D_0\,\mathrm{d}(x, y)(\theta_{y,y} + \nu\theta_{x,x}) \tag{6}$$

$$M_{xy} = \frac{1-\nu}{2} D_0\,\mathrm{d}(x, y)(\theta_{x,y} + \theta_{y,x}) \tag{7}$$

in which $D_0 = Eh_0^3/[12(1-\nu^2)]$. Here E = Young's modulus; ν = Poisson's ratio. On the other hand, the stiffness coefficient, $\mathrm{d}(x, y)$, is defined as

$$\mathrm{d}(x, y) = 1 - \alpha_{i,j} D(x - x_i) D(y - y_j) \tag{8}$$

in which $\alpha_{i,j}$ is defined as

$$\alpha_{i,j} = \left(\frac{h_{i,j}}{h_0}\right)^3 \tag{9}$$

and $D(x-x_i)$ and $D(y-y_j)$ are the specific functions proposed by Takabatake (1991a). The function $D(x-x_i)$ is defined as a function where the Dirac function $\delta(x-\xi)$ exists continuously in the x direction through the i,jth void, namely the region from $x_i-b_{xi,j}/2$ to $x_i+b_{xi,j}/2$, in which ξ can take values from $x_i-b_{xi,j}/2$ to $x_i+b_{xi,j}/2$. Similarly, the function $D(y-y_j)$ is defined as a function where the Dirac function $\delta(y-\eta)$ exists continuously in the y direction through the i,jth void, in which η can take values from $y_j-b_{yi,j}/2$ to $y_j+b_{yi,j}/2$. The use of the specific functions used here makes current formulation and calculation simple.

Meanwhile, the transverse shear forces can be written as

$$Q_x = \kappa_x G_x h_0 (w_{,x}+\theta_x) \tag{10}$$

$$Q_y = \kappa_y G_y h_0 (w_{,y}+\theta_y) \tag{11}$$

The factors, κ_x and κ_y, have been included to account for the nonuniformity of the shear strains over the cross section. The transverse shear stiffnesses, $\kappa_x G_x h_0$ and $\kappa_y G_y h_0$, are determined from both the frame deformation and the transverse shear deformation of the plate elements, as shown in the following section. Hence, (4) becomes

$$U = \frac{1}{2}\int\int\left\{D_0\,\mathrm{d}\left[(\theta_{x,x})^2+2\nu\theta_{x,x}\theta_{y,y}+(\theta_{y,y})^2+\frac{1-\nu}{2}(\theta_{x,y}+\theta_{y,x})^2\right]\right.$$
$$\left.+\kappa_x G_x h_0 (w_{,x}+\theta_x)^2+\kappa_y G_y h_0 (w_{,y}+\theta_y)^2\right\}\mathrm{d}x\,\mathrm{d}y. \tag{12}$$

Next, the variation of the potential of external lateral loads is

$$\delta V = -\int\int p(x,y,t)\delta w\,\mathrm{d}x\,\mathrm{d}y+\int\int c\dot{w}\delta w\,\mathrm{d}x\,\mathrm{d}y-\int_c [m_x^*\delta\theta_x+m_{xy}^*\delta\theta_y]_0^{l_x}\,\mathrm{d}y$$
$$-\int_c [m_y^*\delta\theta_y+m_{yx}^*\delta\theta_x]_0^{l_y}\,\mathrm{d}x-\int_c [q_x^*\delta w]_0^{l_x}\,\mathrm{d}y-\int_c [q_y^*\delta w]_0^{l_y}\,\mathrm{d}x \tag{13}$$

in which p = lateral load; q_x^*, m_x^*, and m_{xy}^* = external transverse force, external moment, and external twisting moment, respectively, prescribed on the mechanical boundary edges at $x=0$ and $x=l_x$; q_y^*, m_y^*, and m_{yx}^* are external transverse forces, external moment, and external twisting moment, respectively, prescribed on the mechanical boundary edges at $y=0$ and $y=l_y$.

The kinetic energy T may be written as

$$T = \frac{1}{2}\int\int\{I_p(x,y)[(\dot{\theta}_x)^2+(\dot{\theta}_y)^2]+m_0\alpha_h(x,y)(\dot{w})^2\}\,\mathrm{d}x\,\mathrm{d}y \tag{14}$$

in which the dot indicates differentiation with respect to time; and the notations, α_h, m_0, and I_p, are defined as

$$\alpha_h = 1-\frac{h_{i,j}}{h_0}D(x-x_i)D(y-y_j) \tag{15}$$

$$m_0 = \rho h_0 \tag{16}$$

$$I_p = \frac{\rho h_0^3}{12} \mathrm{d}(x, y) \tag{17}$$

in which ρ = the mass density of the plate.

Substituting (12)–(14) into the Hamilton's principle, the differential equation of motion can be obtained as

$$\delta w: \quad m_0 \alpha_h \ddot{w} - [\kappa_x G_x h_0 (w_{,x} + \theta_x)]_{,x} - [\kappa_y G_y h_0 (w_{,y} + \theta_y)]_{,y} - p + c\dot{w} = 0 \tag{18}$$

$$\delta\theta_x: \quad I_p \ddot{\theta}_x + \kappa_x G_x h_0 (w_{,x} + \theta_x) - [D_0 d(\theta_{x,x} + \nu\theta_{y,y})]_{,x} - \frac{1-\nu}{2}[D_0 d(\theta_{x,y} + \theta_{y,x})]_{,y} = 0 \tag{19}$$

$$\delta\theta_y: \quad I_p \ddot{\theta}_y + \kappa_y G_y h_0 (w_{,y} + \theta_y) - [D_0 d(\theta_{y,y} + \nu\theta_{x,x})]_{,y} - \frac{1-\nu}{2}[D_0 d(\theta_{x,y} + \theta_{y,x})]_{,x} = 0 \tag{20}$$

together with the associated boundary conditions

$$w = w^* \quad \text{or} \quad \kappa_x G_x h_0 (w_{,x} + \theta_x) = q_x^* \tag{21}$$

$$\theta_x = \theta_x^* \quad \text{or} \quad D_0 d(\theta_{x,x} + \nu\theta_{y,y}) = m_x^* \tag{22}$$

$$\theta_y = \theta_y^* \quad \text{or} \quad \frac{1-\nu}{2} D_0 d(\theta_{x,y} + \theta_{y,x}) = m_{xy}^* \tag{23}$$

at $x = 0$ and l_x; and

$$w = w^* \quad \text{or} \quad \kappa_y G_y h_0 (w_{,y} + \theta_y) = q_y^* \tag{24}$$

$$\theta_x = \theta_x^* \quad \text{or} \quad \frac{1-\nu}{2} D_0 d(\theta_{x,y} + \theta_{y,x}) = m_{yx}^* \tag{25}$$

$$\theta_y = \theta_y^* \quad \text{or} \quad D_0 d(\theta_{y,y} + \nu\theta_{x,x}) = m_y^* \tag{26}$$

at $y = 0$ and l_y, in which w^*, θ_x^*, and θ_y^* = displacement components prescribed on the geometrical boundary.

For solid plates without voids, α_h and d become 1; and the governing equations proposed here reduce to Washizu (1982) and Mindlin's equations (1951) with the transverse shear deformation excluding the frame deformation. Furthermore, neglecting the transverse shear deformation, the governing equations proposed here reduce to the general equations proposed by Takabatake (1991a) for a rectangular plate with relative small voids excluding the transverse shear deformation.

3. TRANSVERSE SHEAR STIFFNESS OF CELLULAR PLATES

The bending and transverse shear stiffnesses of cellular plates decrease due to voids. The former reduction is already considered by the stiffness coefficient d given in (8). On the other hand, the latter reduction is determined from the frame deformation and the transverse shear deformation of the top and bottom platelets and of partitions surrounding a void.

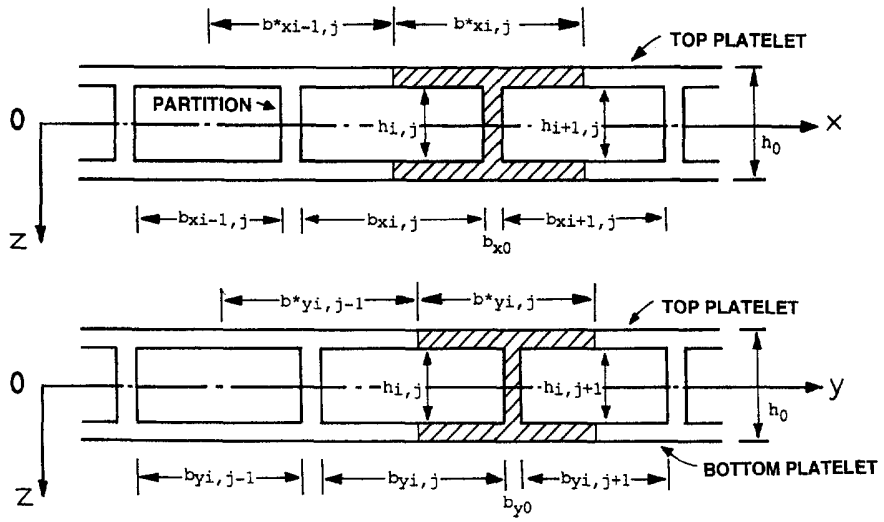

Fig. 3. Cross-section of cellular plates.

Consider the transverse shear stiffness of a cellular plate, as shown in Fig. 3. Assuming that the influence points of top and bottom platelets and of partitions surrounding a void are situated on the midspan of each member, the transverse shear stiffness, $\kappa_x G_x h_0$, per unit width in x direction of the cellular plate is obtained easily from eqn (72) in Takabatake *et al.* (1993a, 1993b) by

$$\kappa_x G_x h_0 = \frac{1}{\dfrac{b^*_{xi,j}\left(\dfrac{b^*_{xi,j}}{I_{c1}+I_{c2}}+\dfrac{h_0}{I_b}\right)}{12E}+\dfrac{1}{\kappa_0 G_0(h_0-h_{i,j})}+\dfrac{b^*_{xi,j}}{\kappa_0 G_0 h_0 b_{x0}}}. \tag{27}$$

This equation is also obtained by adding the shear deformation of members, such as platelets and partition, to the equation given by Smith *et al.* (1984). In (27) the first term of denominator in the right side indicates the frame deformation; the second and third terms indicate the shear deformations of only the top and bottom platelets and of partitions in current voided plate, respectively. The notations, I_{c1}, I_{c2}, and I_b, are defined as

$$I_{c1} = I_{c2} = \frac{1}{24}\left[\left(\frac{h_0-h_{i,j}}{2}\right)^3+\left(\frac{h_0-h_{i+1,j}}{2}\right)^3\right] \tag{28a}$$

$$I_b = \frac{b^3_{x0}}{12} \tag{28b}$$

κ_0 has been included to account for the nonuniformity of the shear strains over the members.

If the void is surrounded by partitions like shear wall, as shown in Fig. 4, the transverse shear stiffnesses for cellular plates must be added the transverse shear stiffness of paralleled partitions (like shear-walls) to the transverse shear stiffness, $(\kappa_x G_x h_0)^*$, given by (27). Hence

$$\kappa_x G_x h_0 = (\kappa_x G_x h_0)^* + \kappa_0 G_0 h_0 \frac{b_{y0}}{b^*_{yi,j}}. \tag{29}$$

When a void passes through in the x direction, as shown in Fig. 5, the transverse shear stiffness in the x direction of the cellular plate is based on only the shear stiffness of the paralleled partitions as the shear walls and is written as

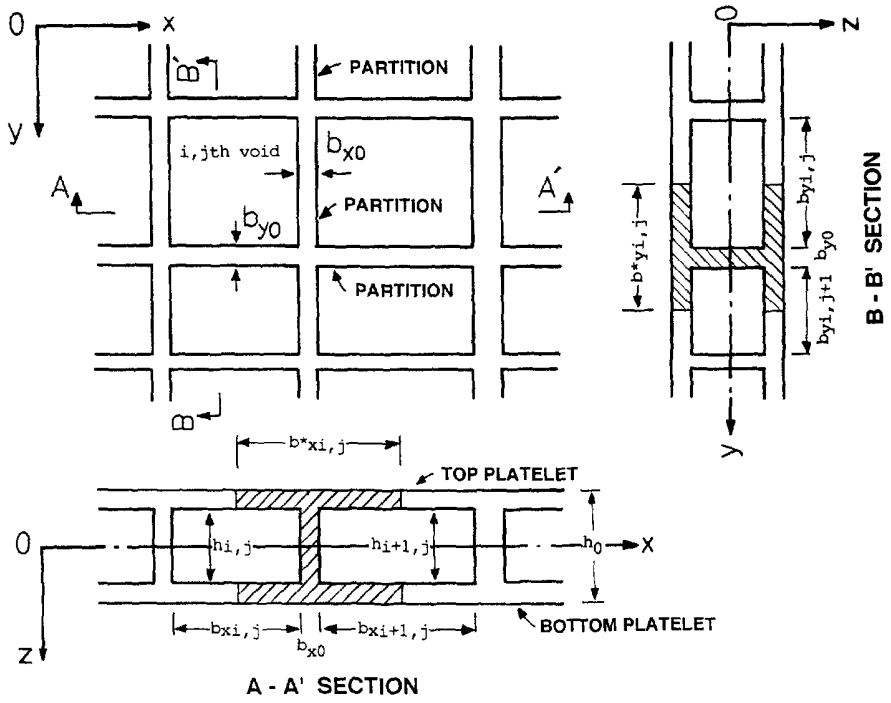

Fig. 4. Cellular plate with crossed partitions.

$$\kappa_x G_x h_0 = \kappa_0 G_0 h_0 \frac{b_{y0}}{b^*_{yi,j}}. \tag{30}$$

Similarly, the transverse shear stiffness, $\kappa_y G_y h_0$, may be written by replacing b_{x0}, $b^*_{xi,j}$, and $b^*_{yi,j}$ with b_{y0}, b_{x0}, $b^*_{yi,j}$, in the mentioned expressions of $\kappa_x G_x h_0$ and $b^*_{xi,j}$, respectively. Thus, the transverse shear stiffness of cellular plates has been presented. It must be noticed that the method proposed here replaces the transverse shear stiffness of the cellular plate in

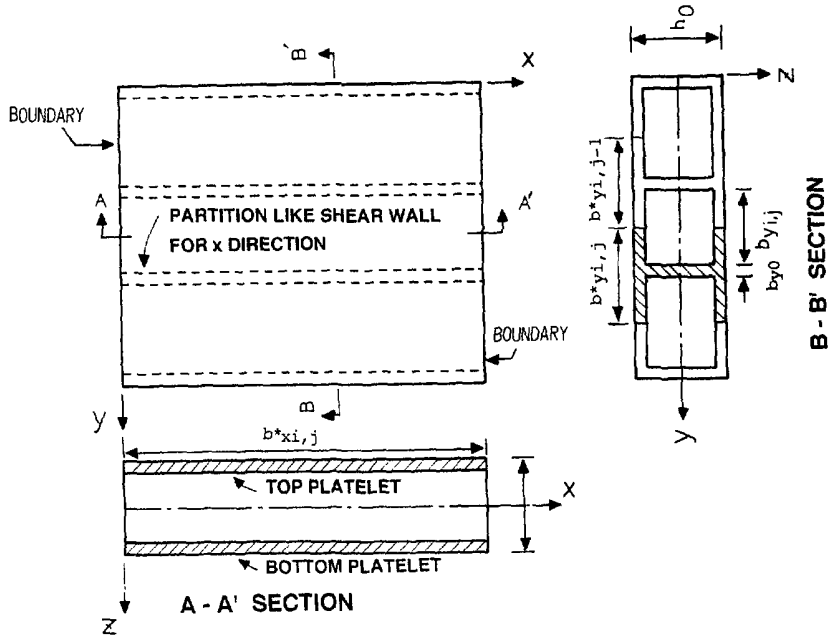

Fig. 5. Plate with voids passed through.

a field of the width $b^*_{xi,j}$ or $b^*_{yi,j}$ prescribed by the i, jth void with an equivalent transverse shear stiffness. The equivalent transverse shear stiffnesses per the i, jth void are expressed as

$$\kappa_x G_x h_0 = \alpha_{Gxi,j} \kappa_0 G_0 h_0 \tag{31}$$

$$\kappa_y G_y h_0 = \alpha_{Gyi,j} \kappa_0 G_0 h_0 \tag{32}$$

in which the coefficients, α_{Gx} and α_{Gy}, are defined as

$$\alpha_{Gxi,j} = \frac{\kappa_x G_x h_0}{\kappa_0 G_0 h_0} D(x-\hat{x}_i) D(y-\hat{y}_j) \tag{33}$$

$$\alpha_{Gyi,j} = \frac{\kappa_y G_y h_0}{\kappa_0 G_0 h_0} D(x-\hat{x}_i) D(y-\hat{y}_j) \tag{34}$$

in which $\hat{x}_i$ and $\hat{y}_j$ indicate the fields (from $x_i - b^*_{xi-1,j}/2$ to $x_i + b^*_{xi,j}/2$ and from $y_j - b^*_{yi,j-1}/2$ to $y_j + b^*_{yi,j}/2$, respectively) prescribed by the i, jth void. For solid plates or a portion without voids, α_{Gx} and α_{Gy} become 1.

4. STRESS RESULTANTS AND STRESS COUPLES OF PLATELETS AND PARTITION

Once the transverse shear forces Q_x and Q_y are obtained, the stress resultants and stress couples of the frame and partition parallel to the x direction, as shown in Fig. 6, given as follows: the transverse shear forces Q_{xframe} and $Q_{xpartition}$ of the frame and partition located parallel to the x direction are

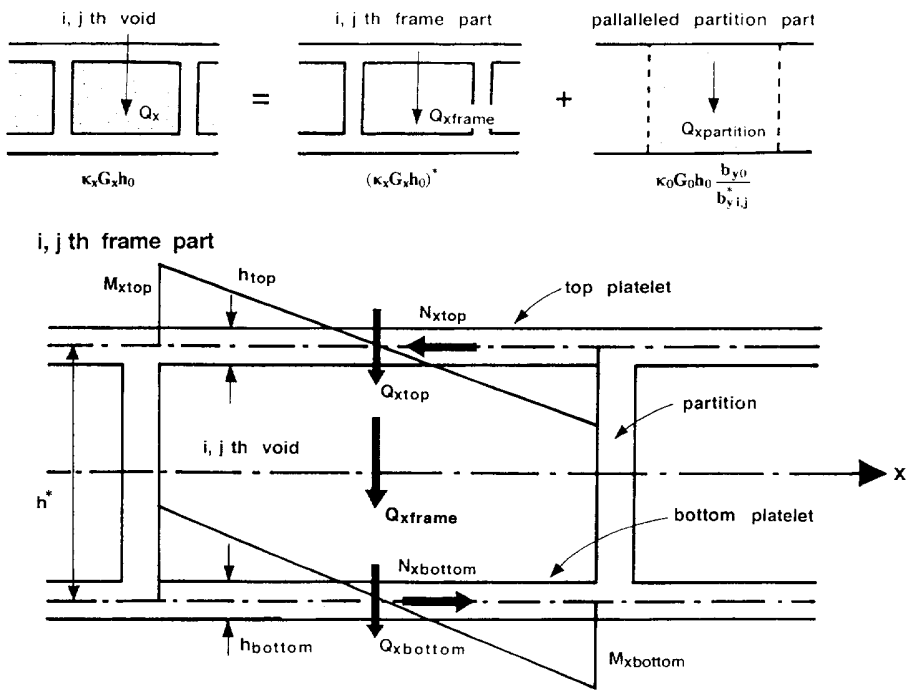

Fig. 6. Stress resultants and stress couples of top and bottom platelets.

$$Q_{xframe} = Q_x \frac{(\kappa_x G_x h_0)^*}{\kappa_x G_x h_0} \tag{35}$$

$$Q_{xpartition} = Q_x \frac{\kappa_0 G_0 h_0}{\kappa_x G_x h_0} \frac{b_{y0}}{b^*_{yi,j}} \tag{36}$$

in which the frame is composed of the top and bottom platelets and of partition per void and excludes the partition parallel like shear wall to the direction. The transverse shear force Q_x is divided by the transverse shear forces Q_{xtop} and $Q_{xbottom}$ of the top and bottom platelets in proportion to the thickness as

$$Q_{xtop} = Q_{xframe} \frac{h_{top}}{h_{top} + h_{bottom}} \tag{37}$$

$$Q_{xbottom} = Q_{xframe} \frac{h_{bottom}}{h_{top} + h_{bottom}} \tag{38}$$

in which h_{top} and h_{bottom} = the slab's thickness of the top and bottom platelets, respectively. Hence, the flexural moments M_{xtop} and $M_{xbottom}$ of the top and bottom platelets at both ends of the i, jth void are given by

$$M_{xtop} = Q_{xtop} \frac{b_{xi,j}}{2} \tag{39}$$

$$M_{xbottom} = Q_{xbottom} \frac{b_{xi,j}}{2}. \tag{40}$$

Lastly, the axial forces $N_{xtop}(= N_{xbottom})$ of the top and bottom platelets, due to the flexural moments, are calculated by

$$N_{xtop} = \frac{M_x + M_{xtop} + M_{xbottom}}{h^*} \tag{41}$$

in which h^* = distance between middle surfaces of top and bottom platelets. Similar expressions for y direction may be obtained.

5. STATIC ANALYSIS

Consider the static solutions by means of the Galerkin method. The deflections, w, and rotational angles, θ_x and θ_y, can be expressed by a series expansion as follows:

$$w(x, y) = \sum_{m=1} \sum_{n=1} w_{mn} f_{mn}(x, y) \tag{42}$$

$$\theta_x(x, y) = \sum_{m=1} \sum_{n=1} \theta_{xmn} g_{xmn}(x, y) \tag{43}$$

$$\theta_y(x, y) = \sum_{m=1} \sum_{n=1} \theta_{ymn} g_{ymn}(x, y) \tag{44}$$

in which w_{mn}, θ_x, and θ_y = unknown displacement coefficients; and f_{mn}, g_{xmn}, and g_{ymn} = shape functions satisfying the specified boundary conditions.

The Galerkin equations for the static problem can be written as

$$\delta w_{mn}: \quad \sum_{\bar{m}=1}\sum_{\bar{n}=1} w_{\bar{m}\bar{n}} A_{1mn\bar{m}\bar{n}} + \sum_{\bar{m}=1}\sum_{\bar{n}=1} \theta_{x\bar{m}\bar{n}} A_{2mn\bar{m}\bar{n}} + \sum_{\bar{m}=1}\sum_{\bar{n}=1} \theta_{y\bar{m}\bar{n}} A_{3mn\bar{m}\bar{n}} = P_{mn} \tag{45}$$

$$\delta\theta_{xmn}: \quad \sum_{\bar{m}=1}\sum_{\bar{n}=1} w_{\bar{m}\bar{n}} B_{1mn\bar{m}\bar{n}} + \sum_{\bar{m}=1}\sum_{\bar{n}=1} \theta_{x\bar{m}\bar{n}} B_{2mn\bar{m}\bar{n}} + \sum_{\bar{m}=1}\sum_{\bar{n}=1} \theta_{y\bar{m}\bar{n}} B_{3mn\bar{m}\bar{n}} = 0 \tag{46}$$

$$\delta\theta_{ymn}: \quad \sum_{\bar{m}=1}\sum_{\bar{n}=1} w_{\bar{m}\bar{n}} C_{1mn\bar{m}\bar{n}} + \sum_{\bar{m}=1}\sum_{\bar{n}=1} \theta_{x\bar{m}\bar{n}} C_{2mn\bar{m}\bar{n}} + \sum_{\bar{m}=1}\sum_{\bar{n}=1} \theta_{y\bar{m}\bar{n}} C_{3mn\bar{m}\bar{n}} = 0 \tag{47}$$

in which the coefficients $A_{1mn\bar{m}\bar{n}}, \ldots, C_{3mn\bar{m}\bar{n}}$ are given in Appendix I. The unknown displacement coefficients are obtained from solving a set of algebraic linear equations given by (45)–(47).

6. NUMERICAL RESULTS FOR STATIC CALCULATION

Static analysis for a rectangular cellular plate has been presented by means of the Galerkin method. Then, to examine the proposed method, numerical calculations are performed for two types of simply-supported and clamped cellular plates, as shown in Table 1. Data used are as follows: the Young's modulus $E = 2.059 \times 10^{10}$ Pa; Poisson's ratio $\nu = 0.17$; slab's height $h_0 = 1$ m; span lengths $l_x = l_y = 30$ m; void's height $h_{i,j} = 0.8$ m. For simplicity, the lateral load is assumed to be uniformly distributed load $p = 9.807 \times 10^6$ Pa; mass density $\rho = 244.9$ kg/m^3.

The shape functions used are

$$f_{mn}(x, y) = \sin\frac{m\pi x}{l_x}\sin\frac{n\pi y}{l_y} \tag{48}$$

$$g_{xmn}(x, y) = \cos\frac{m\pi x}{l_x}\sin\frac{n\pi y}{l_y} \tag{49}$$

$$g_{ymn}(x, y) = \sin\frac{m\pi x}{l_x}\cos\frac{n\pi y}{l_y} \tag{50}$$

for the simply-supported plates and

$$f_{mn}(x, y) = \bar{x}^m(\bar{x}^2 - 1)\bar{y}^n(\bar{y}^2 - 1) \tag{51}$$

$$g_{xmn}(x, y) = \bar{x}^{m+1}(\bar{x}^2 - 1)\bar{y}^n(\bar{y}^2 - 1) \tag{52}$$

Table 1. Lists of isotropic rectangular cellular plates

Type	Plane	Section	$h_{i,j}$	$b_{xi,j}$	$b_{yi,j}$
P1		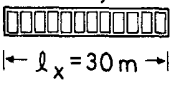	0.8	2.3	30.0
P2			0.8	2.4	30.0
P3		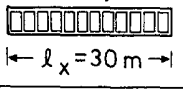	0.8	2.3	2.3
P4			0.8	2.4	2.4

unit : m

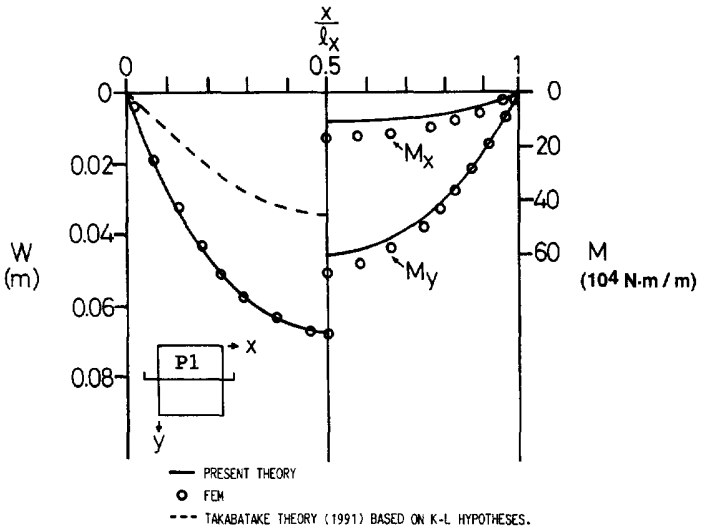

Fig. 7. w and M_y for a simply-supported cellular plate.

$$g_{ymn}(x, y) = \bar{x}^m(\bar{x}^2 - 1)\bar{y}^{n+1}(\bar{y}^2 - 1) \tag{53}$$

for the clamped plate, in which $\bar{x}$ and $\bar{y}$ are defined as $\bar{x} = 2x/l_x$ and $\bar{y} = 2y/l_y$, respectively.

Figures 7 and 8 show the deflections, w, and bending moments, M_x and M_y, for the simply-supported and clamped plates. In these figures the solid lines indicate the numerical results obtained from the proposed theory; the circles indicate the numerical results obtained by using FEM code NASTRAN; the broken lines indicate the numerical results obtained from Takabatake's theory (1991a) excluding the transverse shear deformation. The results obtained from the theory proposed here show relatively good agreement with the results obtained from the finite element method. The finite element method used here is based on isotropic and rectangular plate elements proposed on the top and bottom platelets and partitions of the voids, as shown in Fig. 9. The result obtained from the plate element used here in FEM are confirmed to show excellent agreement with the result using solid element to current plates.

Figure 10 shows the transverse shear forces, flexural moments, and axial forces of top and bottom platelets at adjacent midspan for clamped cellular plate P2. Figure 11 indicates

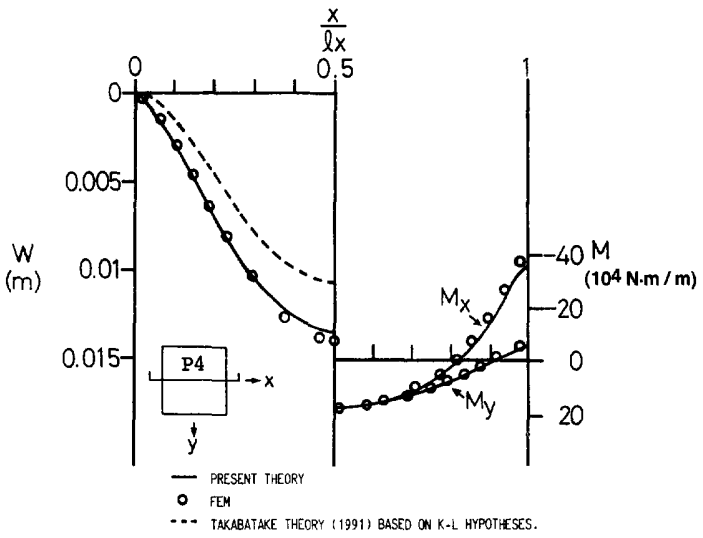

Fig. 8. w and M_y for a clamped cellular plate.

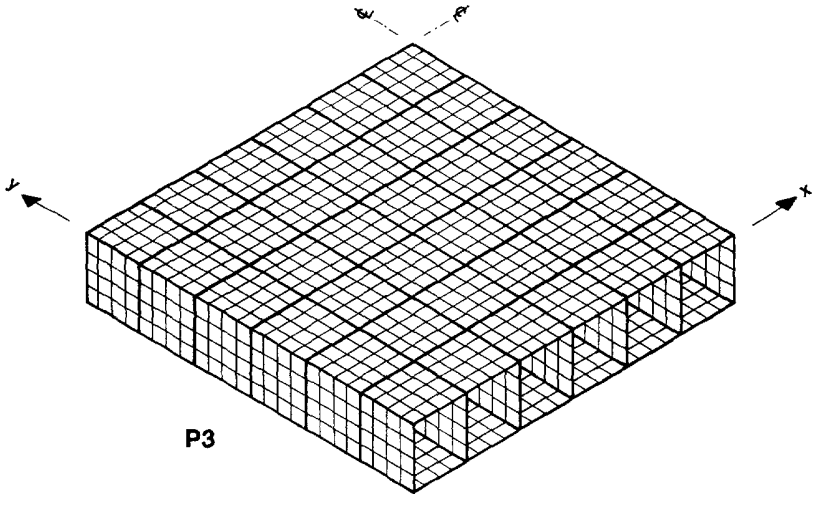

Fig. 9. Mesh of FEM.

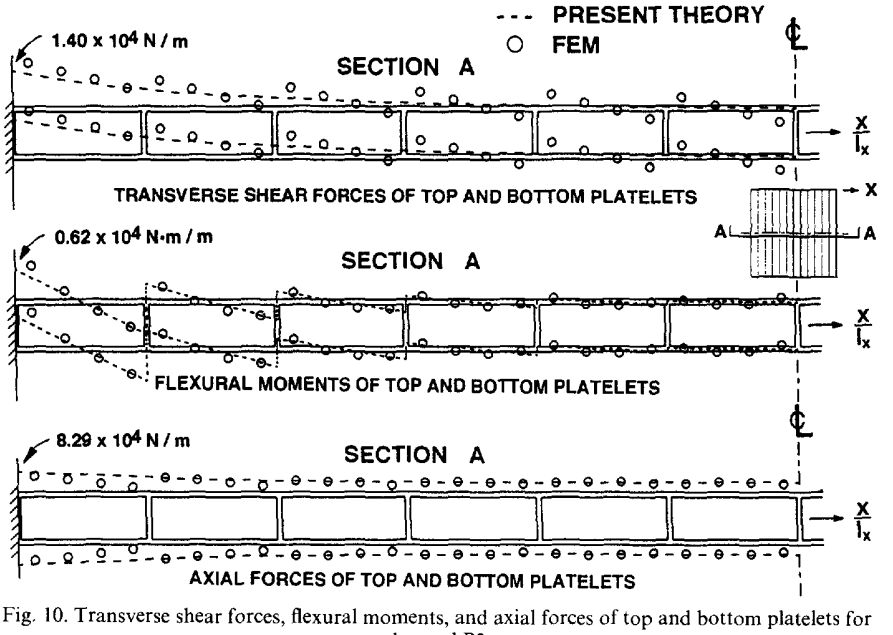

Fig. 10. Transverse shear forces, flexural moments, and axial forces of top and bottom platelets for clamped P2.

the flexural moment of partition and the axial forces of top and bottom platelets for the same cellular plate. It is clarified from these figures that the simplified theory proposed here also shows agreement with the results using the finite element method. For the other plates a similar good agreement is obtained.

The convergence of series expansion is very rapid for uniform loads. So, the consideration of 16 terms gives an accuracy sufficient for all practical purposes.

7. FREE TRANSVERSE VIBRATIONS OF CELLULAR PLATES

Consider free transverse vibrations of a cellular plate. The method of separation of variables is employed, assuming that

$$w(x, y, t) = \bar{w}(x, y)e^{i\omega t}(t) \tag{54}$$

$$\theta_x(x, y, t) = \bar{\theta}_x(x, y)e^{i\omega t}(t) \tag{55}$$

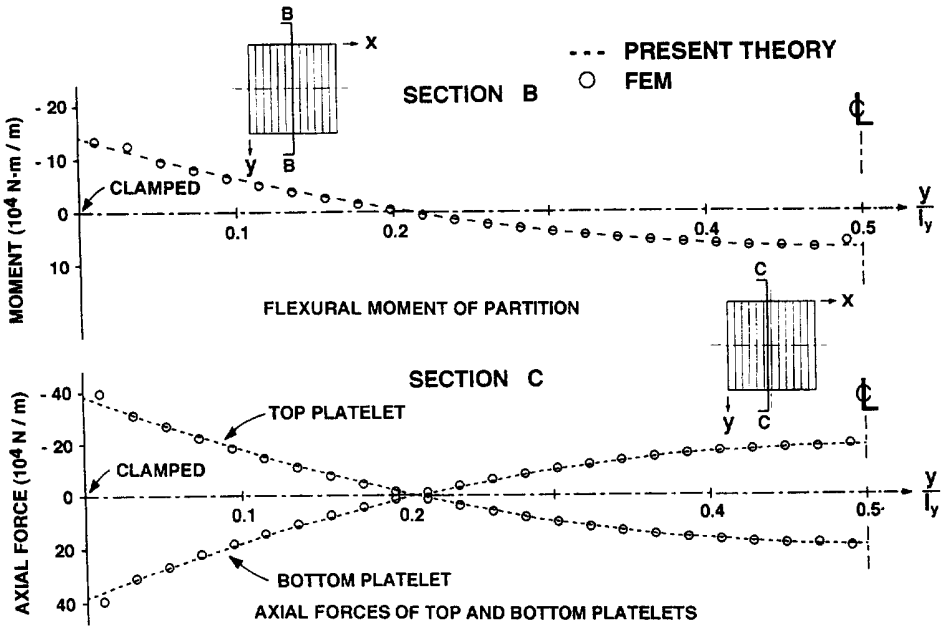

Fig. 11. Flexural moment of partition and axial forces of top and bottom platelets for clamped P2.

$$\theta_y(x, y, t) = \bar{\theta}_y(x, y)e^{i\omega t}(t) \tag{56}$$

in which $\bar{w}$, $\bar{\theta}_x$ and $\bar{\theta}_y$ = functions of x and y. Hence, free transverse vibrations obtained from (18)–(20) become

$$\delta w: \quad \omega^2 m_0 \alpha_h \bar{w} + [\kappa_x G_x h_0(\bar{w}_{,x} + \bar{\theta}_x)]_{,x} + [\kappa_y G_y h_0(\bar{w}_{,y} + \bar{\theta}_y)]_{,y} = 0 \tag{57}$$

$$\delta\theta_x: \quad -\omega^2 I_p \bar{\theta}_x + \kappa_x G_x h_0(\bar{w}_{,x} + \bar{\theta}_x) - [D_0 d(\bar{\theta}_{x,x} + \nu\bar{\theta}_{y,y})]_{,x} - \frac{1-\nu}{2}[D_0 d(\bar{\theta}_{x,y} + \bar{\theta}_{y,x})]_{,y} = 0 \tag{58}$$

$$\delta\theta_y: \quad -\omega^2 I_p \bar{\theta}_y + \kappa_y G_y h_0(\bar{w}_{,y} + \bar{\theta}_y) - [D_0 d(\bar{\theta}_{y,y} + \nu\bar{\theta}_{x,x})]_{,y} - \frac{1-\nu}{2}[D_0 d(\bar{\theta}_{x,y} + \bar{\theta}_{y,x})]_{,x} = 0 \tag{59}$$

in which ω = a constant.

The natural frequencies are presented by means of the Galerkin method. $\bar{w}$, $\bar{\theta}_x$, and $\bar{\theta}_y$ are expressed as

$$\bar{w}(x, y) = w_{mn} f_{mn}(x, y) \tag{60}$$

$$\bar{\theta}_x(x, y) = \theta_{xmn} g_{xmn}(x, y) \tag{61}$$

$$\bar{\theta}_y(x, y) = \theta_{ymn} g_{ymn}(x, y) \tag{62}$$

in which w_{mn}, θ_{xmn}, and θ_{ymn} = unknown displacement coefficients; and f_{mn}, g_{xmn}, and g_{ymn} = shape functions satisfying the specified boundary conditions. Hence, the Galerkin equations of (57)–(59) become

$$\delta w_{mn}: \quad w_{\bar{m}\bar{n}}(A_{1mn\bar{m}\bar{n}}+\omega^2 m_0 F_{1mn\bar{m}\bar{n}})+\theta_{x\bar{m}\bar{n}}A_{2mn\bar{m}\bar{n}}+\theta_{y\bar{m}\bar{n}}A_{3mn\bar{m}\bar{n}}=0 \tag{63}$$

$$\delta\theta_{xmn}: \quad w_{\bar{m}\bar{n}}B_{1mn\bar{m}\bar{n}}+\theta_{x\bar{m}\bar{n}}(B_{2mn\bar{m}\bar{n}}-\omega^2 F_{2mn\bar{m}\bar{n}})+\theta_{y\bar{m}\bar{n}}B_{3mn\bar{m}\bar{n}}=0 \tag{64}$$

$$\delta\theta_{ymn}: \quad w_{\bar{m}\bar{n}}C_{1mn\bar{m}\bar{n}}+\theta_{x\bar{m}\bar{n}}C_{2mn\bar{m}\bar{n}}+\theta_{y\bar{m}\bar{n}}(C_{3mn\bar{m}\bar{n}}-\omega^2 F_{3mn\bar{m}\bar{n}})=0 \tag{65}$$

in which $F_{1mn\bar{m}\bar{n}}$, $F_{2mn\bar{m}\bar{n}}$ and $F_{3mn\bar{m}\bar{n}}$ are defined as

$$F_{1mn\bar{m}\bar{n}}=\int_0^{l_x}\int_0^{l_y} f_{\bar{m}\bar{n}}f_{mn}\,\mathrm{d}x\,\mathrm{d}y-\sum_{i=1}\sum_{j=1}\int_0^{l_x}\int_0^{l_y}\left(\frac{h_{i,j}}{h_0}\right)D(x-x_i)D(y-y_j)f_{\bar{m}\bar{n}}f_{mn}\,\mathrm{d}x\,\mathrm{d}y \tag{66}$$

$$F_{2mn\bar{m}\bar{n}}=\frac{\rho h_0^3}{12}\left[\int_0^{l_x}\int_0^{l_y} g_{x\bar{m}\bar{n}}g_{xmn}\,\mathrm{d}x\,\mathrm{d}y-\sum_{i=1}\sum_{j=1}\int_0^{l_x}\int_0^{l_y}\alpha_{i,j}D(x-x_i)D(y-y_j)g_{x\bar{m}\bar{n}}g_{xmn}\,\mathrm{d}x\,\mathrm{d}y\right] \tag{67}$$

$$F_{3mn\bar{m}\bar{n}}=\frac{\rho h_0^3}{12}\left[\int_0^{l_x}\int_0^{l_y} g_{y\bar{m}\bar{n}}g_{ymn}\,\mathrm{d}x\,\mathrm{d}y-\sum_{i=1}\sum_{j=1}\int_0^{l_x}\int_0^{l_y}\alpha_{i,j}D(x-x_i)D(y-y_j)g_{y\bar{m}\bar{n}}g_{ymn}\,\mathrm{d}x\,\mathrm{d}y\right]. \tag{68}$$

The natural frequencies ω_{mn} are obtained by solving (63)–(65) as eigenvalue problems for a prescribed value of $m=\bar{m}$ and $n=\bar{n}$.

Then, for practical uses, approximate expressions for the natural frequencies are considered. Expressing θ_{xmn} and θ_{ymn} in terms of w_{mn} and ω^2 from (63)–(65) and neglecting the terms of $(\omega^2)^2$ and $(\omega^2)^3$ in a cubic equation with respect to ω^2, the m, nth natural frequency ω_{mn} is obtained as

$$\omega_{mn}\approx\sqrt{\frac{K_{mn}}{F_{mn}}} \tag{69}$$

in which K_{mn} and F_{mn} are defined as

$$K_{mn}=A_{1mnmn}(-B_{2mnmn}C_{3mnmn}+B_{3mnmn}C_{2mnmn})+A_{2mnmn}(B_{1mnmn}C_{3mnmn}-C_{1mnmn}B_{3mnmn})$$
$$+A_{3mnmn}(C_{1mnmn}B_{2mnmn}-B_{1mnmn}C_{2mnmn}) \tag{70}$$

$$F_{mn}=A_{1mnmn}(-B_{2mnmn}F_{3mnmn}-C_{3mnmn}F_{2mnmn})+m_0F_{1mnmn}(B_{2mnmn}C_{3mnmn}-B_{3mnmn}C_{2mnmn})$$
$$+A_{2mnmn}B_{1mnmn}F_{3mnmn}+A_{3mnmn}C_{1mnmn}F_{2mnmn}. \tag{71}$$

8. NUMERICAL RESULTS FOR NATURAL FREQUENCIES

The natural frequencies for a rectangular cellular plate have been presented in an approximate form by means of the Galerkin method. Then, to examine the proposed method, numerical computations are performed for the previous rectangular cellular plates, as shown in Table 1. The shape function is made up of the well-known natural functions of beams, for instance as given in Szilard (1974). The current shape functions used are (48)–(50) for simply-supported plates and the following natural function of clamped beams for clamped plate:

Table 2. Natural frequencies of simply supported and clamped cellular plates P1

	(rad/sec)	Simply-supported $m=1$	$m=2$	$m=3$	Clamped $m=1$	$m=2$	$m=3$
$n=1$	RIGOROUS	18.66	29.42	41.34	32.80	41.14	51.34
	APPROXIMATE	18.64	29.39	41.29	32.76	41.10	51.29
	FEM	18.49	28.95	40.92	33.01	40.04	49.63
$n=2$	RIGOROUS	53.42	60.40	73.39	79.66	86.20	95.96
	APPROXIMATE	53.16	61.19	73.42	79.23	85.87	95.64
	FEM	55.69	63.24	74.52	79.39	84.59	92.90
$n=3$	RIGOROUS	111.00	112.70	124.22	145.37	149.64	157.81
	APPROXIMATE	109.58	114.16	124.17	143.40	148.17	156.51
	FEM	110.72	113.35	126.77	138.80	142.67	158.90

In which m = mode number in x-direction, n = mode number in y-direction.

$$f_{mn}(x,y) = \left\{\mathrm{ch}\left(\frac{\lambda_m x}{l_x}\right) - \cos\left(\frac{\lambda_m x}{l_x}\right) - \frac{\mathrm{ch}\,\lambda_m - \cos\lambda_m}{\mathrm{sh}\,\lambda_m - \sin\lambda_m}\left[\mathrm{sh}\left(\frac{\lambda_m x}{l_x}\right) - \sin\left(\frac{\lambda_m x}{l_x}\right)\right]\right\}$$
$$\times\left\{\mathrm{ch}\left(\frac{\lambda_n y}{l_y}\right) - \cos\left(\frac{\lambda_n y}{l_y}\right) - \frac{\mathrm{ch}\,\lambda_n - \cos\lambda_n}{\mathrm{sh}\,\lambda_n - \sin\lambda_n}\left[\mathrm{sh}\left(\frac{\lambda_n y}{l_y}\right) - \sin\left(\frac{\lambda_n y}{l_y}\right)\right]\right\} \quad (72)$$

in which λ_m and λ_n = well-known constants.

Table 2 shows the natural frequencies for Type P1. It shows that the differences between the results obtained using (63)–(65) and the approximate results obtained using (69) are negligible in practical use. The results obtained from the proposed theory show good agreement with results obtained from FEM. For the other plates a similar agreement is obtained.

9. FORCED VIBRATIONS OF CELLULAR PLATES

Consider forced vibrations of the current rectangular cellular plate. The general solutions of (18)–(20) are assumed to be of the form

$$w(x,y,t) = \sum_{m=1}\sum_{n=1} f_{mn}(x,y)w_{mn}(t) \quad (73)$$

$$\theta_x(x,y,t) = \sum_{m=1}\sum_{n=1} g_{xmn}(x,y)\theta_{xmn}(t) \quad (74)$$

$$\theta_y(x,y,t) = \sum_{m=1}\sum_{n=1} g_{ymn}(x,y)\theta_{ymn}(t) \quad (75)$$

in which w_{mn}, θ_{xmn} and θ_{ymn} = unknown functions of time t.

Then, (18)–(20) may be rewritten as

$$\delta w_{mn}: \quad \sum_{\bar{m}=1}\sum_{\bar{n}=1}(\ddot{w}_{\bar{m}\bar{n}} m_0 F_{1mn\bar{m}\bar{n}} + 2h_{\bar{m}\bar{n}}\omega_{\bar{m}\bar{n}} m_0 \dot{w}_{\bar{m}\bar{n}} F_{1mn\bar{m}\bar{n}}$$
$$- w_{\bar{m}\bar{n}} A_{1mn\bar{m}\bar{n}} - \theta_{x\bar{m}\bar{n}} A_{2mn\bar{m}\bar{n}} - \theta_{y\bar{m}\bar{n}} A_{3mn\bar{m}\bar{n}}) - P_{mn} = 0 \quad (76)$$

$$\delta\theta_{xmn}: \quad \sum_{\bar{m}=1}\sum_{\bar{n}=1}(\ddot{\theta}_{x\bar{m}\bar{n}} F_{2mn\bar{m}\bar{n}} + w_{\bar{m}\bar{n}} B_{1mn\bar{m}\bar{n}} + \theta_{x\bar{m}\bar{n}} B_{2mn\bar{m}\bar{n}} + \theta_{y\bar{m}\bar{n}} B_{3mn\bar{m}\bar{n}}) = 0 \quad (77)$$

$$\delta\theta_{ymn}: \quad \sum_{\bar{m}=1}\sum_{\bar{n}=1}(\ddot{\theta}_{y\bar{m}\bar{n}} F_{3mn\bar{m}\bar{n}} + w_{\bar{m}\bar{n}} C_{1mn\bar{m}\bar{n}} + \theta_{x\bar{m}\bar{n}} C_{2mn\bar{m}\bar{n}} + \theta_{y\bar{m}\bar{n}} C_{3mn\bar{m}\bar{n}}) = 0 \quad (78)$$

in which h_{mn} = damping constant of the cellular plate. The dynamic response is obtained by solving (76)–(78). The coefficients in these equations have non-diagonal terms $m \neq \bar{m}$ and/or $n \neq \bar{n}$ due to the effect of the voids. Therefore, the solution will be based on either numerical computation, such as the Wilson-θ method, or the approximate solution in following section.

10. APPROXIMATE SOLUTIONS FOR FORCED VIBRATIONS

For practical use, consider an approximate solution in the closed-form. Assuming that the behavior of a cellular plate is now dominated by only the diagonal terms in the coefficients, (76)–(78) become of uncoupled form with respect to m and $\bar{m}$, and, n and $\bar{n}$, respectively. Furthermore, neglecting the rotatory inertia's terms in the uncoupled equations, we have the following differential equation in term of only w_{mn}:

$$\ddot{w}_{mn} + 2a_{mn}\dot{w}_{mn} + b_{mn}w_{mn} = Q_{mn}(t) \tag{79}$$

in which

$$a_{mn} \equiv h_{mn}\omega_{mn} \tag{80}$$

$$b_{mn} \equiv -\frac{A^*_{mn}}{m_0 F_{1mnmn}} \tag{81}$$

$$Q_{mn}(t) \equiv \frac{P_{mn}}{m_0 F_{1mnmn}} \tag{82}$$

in which

$$A^*_{mn} = A_{1mnmn} - \frac{1}{\Delta_{mn}}[A_{2mnmn}(C_{3mnmn}B_{1mnmn} - B_{3mnmn}C_{1mnmn}) + A_{3mnmn}(B_{2mnmn}C_{1mnmn} - B_{1mnmn}C_{2mnmn})] \tag{83}$$

where

$$\Delta_{mn} = B_{2mnmn}C_{3mnmn} - B_{3mnmn}C_{2mnmn}. \tag{84}$$

The general solution of (79) is

$$w_{mn} = e^{-a_{mn}t}(C_1 \sin\alpha_{0mn}t + C_2\cos\alpha_{0mn}t) + \frac{1}{\alpha_{0mn}}\int_0^t e^{-a_{mn}(t-\tau)}\sin\alpha_{0mn}(t-\tau)Q_{mn}(\tau)\,d\tau \tag{85}$$

in which C_1 and C_2 = constants; and α_{0mn} are defined as

$$\alpha_{0mn} \equiv \sqrt{b_{mn} - a^2_{mn}}. \tag{86}$$

Thus the dynamic deflections of a rectangular cellular plate are determined by substituting (85) into (73).

11. NUMERICAL RESULTS FOR DYNAMIC RESPONSES

To examine the closed-form approximate solution proposed here, numerical computations are carried out for the previous cellular plates, as shown in Table 1. The damping constants h_{mn} are 0.03 for all modes. The following two types of external lateral loads

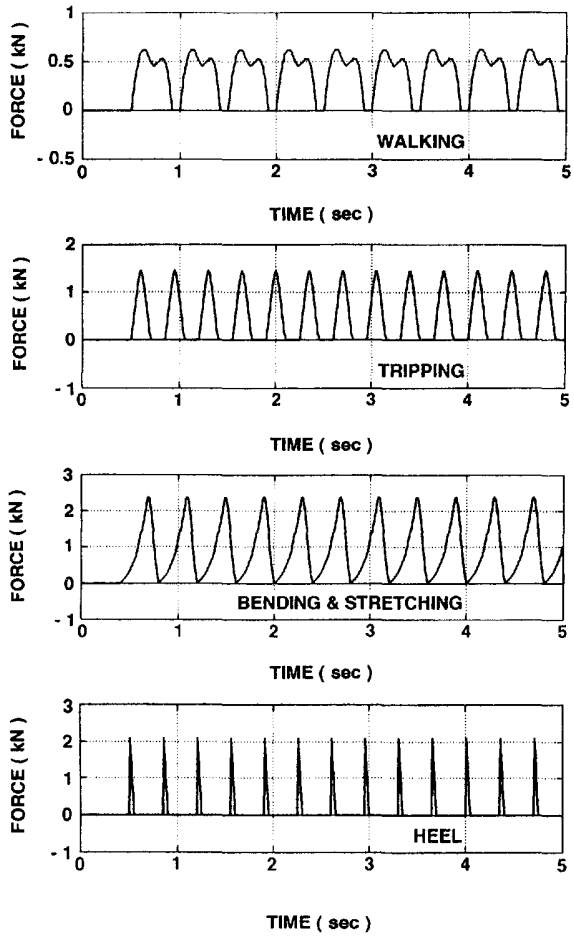

Fig. 12. Test loads for floors.

without the additional mass are assumed: a harmonic and uniformly-distributed force $p = p^* \sin \omega_p t$, in which $p^* = 9.807 \times 10^6$ Pa and $\omega_p = 62.83$ rad/sec (10 cps), and test loads checking the disturbing effect of the vibration of floors caused by people walking and other every usage, as shown in Fig. 12. The test loads consists of four types of walking, tripping, bending and stretching, and heel. They act as a concentrated load at the midspan. The current natural functions used are the same ones as used in the free vibrations.

Figure 13 shows the dynamic deflections at the midpoint of simply supported cellular plates of Type $P1$ subjected to the harmonic load. In this figure, the solid lines indicate values obtained from the numerical computations using the linear acceleration method; the broken lines indicate values obtained from the approximate solution; and the solid lines with circles indicate values obtained from FEM. The difference between solid lines and broken lines is too small to plot. Table 3 shows the maximum dynamic deflections at the midspan of the cellular plates subjected to the harmonic load. Figure 14 shows the dynamic deflections at the midpoint of clamped cellular plates of P4, subjected to the test loads. The numerical results show that the approximate solution proposed here is applicable to the dynamic analyses of cellular plates, in practical use.

For these numerical models the calculations using the present theory are remarkably fast as compared to those using FEM. For example CPU time of P4 for the harmonic load using the present theory with Work Station HP 715/50 is about 40 seconds; and the input

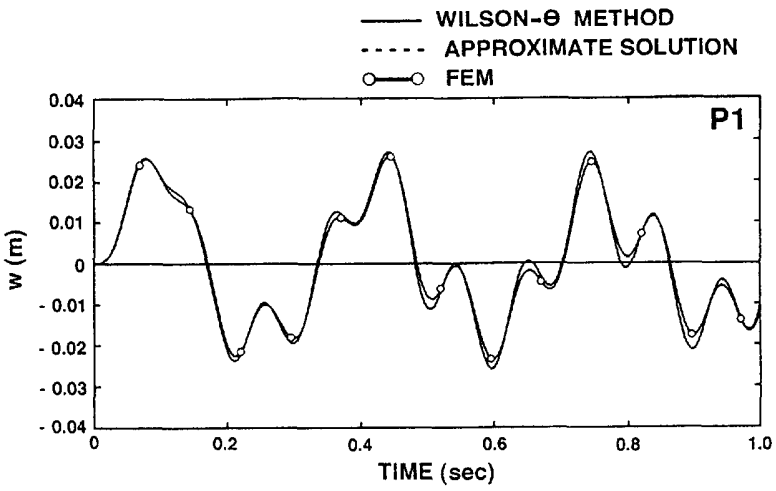

Fig. 13. Dynamic deflections of a simply-supported plate P1 subjected to uniform load.

Table 3. Maximum dynamic deflection of cellular plates

		Maximum dynamic deflection	
Type	Analytical method	Simply supported	Clamped
	Wilson-θ Method	0.02723 m	0.01875 m
P1	Approximate Solution	0.02715 m	0.02223 m
	FEM	0.02624 m	0.01874 m
	Wilson-θ Method	0.03964 m	0.02608 m
P2	Approximate Solution	0.03971 m	0.02923 m
	FEM		0.02455 m
	Wilson-θ Method	0.02247 m	0.02279 m
P3	Approximate Solution	0.02291 m	0.02281 m
	FEM	0.02111 m	0.02156 m
	Wilson-θ Method	0.02730 m	0.02731 m
P4	Approximate Solution	0.02733 m	0.02905 m
	FEM		0.02638 m

data are very simple. Since the series in the theory proposed here converges very rapidly, the consideration of nine terms gives an accuracy sufficient for all practical purpose.

12. CONCLUSIONS

The general and simplified analysis methods for an isotropic rectangular cellular plate with arbitrarily-disposed voids have been proposed by considering the transverse shear deformation along with frame deformation. It is clarified from numerical computations that the simplified theory proposed here is usable in the preliminary stage of designs of such a cellular plate.

Acknowledgments—The authors would like to express their appreciation to T. Ishihara of Nihon-Kokudo-Kaihatsu Corporation and A. Tamatsukuri of Chizaki Corporation for their help in the computations.

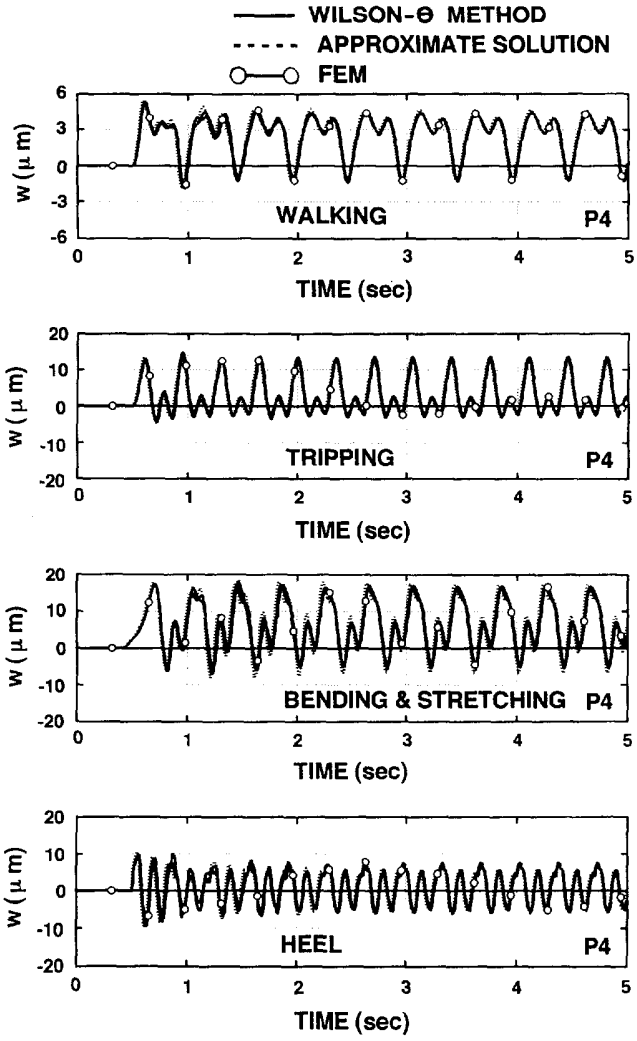

Fig. 14. Dynamic deflections of a clamped plate P4 subjected to test loads.

REFERENCES

Cope, R. J., Harris, G. and Sawko, F. (1973). A new approach to the analysis of cellular bridge decks. *Analysis Struct. Systems for Torsion, ACI*, **35**, 185–210.

Crisfield, M. A. and Twemlow, R. P. (1971). The equivalent plate approach for the analysis of cellular structures. *Civil Engng & Public Works Rev.*, March, 259–263.

Elliott, G. (1978). Partial loading on orthotropic plates. *Cement and Concrete Association Technical Report* 42, p. 519, London.

Holmberg, A. (1960). *Shear-weak Beams on Elastic Foundation*, Vol. 10. International Association for Bridge and Structural Engineering (IABSE), Zurich.

Mindlin, R. D. (1951). Influence of rotatory inertia and shear on flexural motions of isotropic, elastic plates. *J. Appl. Mech. ASME* **18**, 31–38.

Reissner, E. (1945). The effect of transverse shear deformation on the bending of elastic plates. *J. Appl. Mech.* **12**, A69–77.

Sawko, F. and Cope, R. J. (1969). Analysis of multi-cell bridges without transverse diaphragms-a finite element approach. *The Structural Engineer* **47**, 455–460.

Smith, B. S., Kuster, M., and Hoenderkamp, J. C. D. (1984). Generalized method for estimating drift in high-rise structures. *J. Struct. Engng, ASCE* **110**, 1549–2072.

Szilard, R. (1974). *Theory and Analysis of Plates*. Prentice-Hall, Englewood Cliffs, New Jersey.

Takabatake, H. (1988). Lateral buckling of I beams with web stiffeners and batten plates. *Int. J. Solids Structures* **24**, 1003–1019.

Takabatake, H. (1991a). Static analyses of elastic plates with voids. *Int. J. Solids Structures* **28**, 179–196.

Takabatake, H. (1991b). Dynamic analyses of elastic plates with voids. *Int. J. Solids Structures* **28**, 879–895.

Takabatake, H., Mukai, H. and Hirano, T. (1993a). Doubly symmetric tube structures. I : static analysis. *J. Struc. Engng., ASCE* **119**, 1981–2001.

Takabatake, H., Mukai, H. and Hirano, T. (1993b). Doubly symmetric tube structures. II : Dynamic analysis. *J. Struct. Engng., ASCE* **119**, 2002–2016.

Washizu, K. (1982). *Variational Methods in Elasticity and Plasticity*, 3rd Edn. Pergamon Press, New York, N.Y.

APPENDIX 1. COEFFICIENTS AND LOAD TERMS

The coefficients are defined as

$$A_{1mn\bar{m}\bar{n}} = \kappa_0 G_0 h_0 \int_0^{l_x}\int_0^{l_y} [(\alpha_{Gx} f_{\bar{m}\bar{n},x})_{,x} + (\alpha_{Gy} f_{\bar{m}\bar{n},y})_{,y}] f_{mn}\,\mathrm{d}x\,\mathrm{d}y \tag{A1}$$

$$A_{2mn\bar{m}\bar{n}} = \kappa_0 G_0 h_0 \int_0^{l_x}\int_0^{l_y} (\alpha_{Gx} g_{x\bar{m}\bar{n}})_{,x} f_{mn}\,\mathrm{d}x\,\mathrm{d}y \tag{A2}$$

$$A_{3mn\bar{m}\bar{n}} = \kappa_0 G_0 h_0 \int_0^{l_x}\int_0^{l_y} (\alpha_{Gy} g_{y\bar{m}\bar{n}})_{,y} f_{mn}\,\mathrm{d}x\,\mathrm{d}y \tag{A3}$$

$$B_{1mn\bar{m}\bar{n}} = \kappa_0 G_0 h_0 \int_0^{l_x}\int_0^{l_y} \alpha_{Gx,x} f_{\bar{m}\bar{n},x} g_{xmn}\,\mathrm{d}x\,\mathrm{d}y \tag{A4}$$

$$B_{2mn\bar{m}\bar{n}} = \int_0^{l_x}\int_0^{l_y} \left[\kappa_0 G_0 h_0 \alpha_{Gx} g_{x\bar{m}\bar{n}} - D_0 (d g_{x\bar{m}\bar{n},x})_{,x} - \frac{1-\nu}{2} D_0 (d g_{x\bar{m}\bar{n},y})_{,y}\right] g_{xmn}\,\mathrm{d}x\,\mathrm{d}y \tag{A5}$$

$$B_{3mn\bar{m}\bar{n}} = D_0 \int_0^{l_x}\int_0^{l_y} \left[-\nu (d g_{y\bar{m}\bar{n},y})_{,x} - \frac{1-\nu}{2} (d g_{y\bar{m}\bar{n},x})_{,y}\right] g_{xmn}\,\mathrm{d}x\,\mathrm{d}y \tag{A6}$$

$$C_{1mn\bar{m}\bar{n}} = \kappa_0 G_0 h_0 \int_0^{l_x}\int_0^{l_y} \alpha_{Gx} f_{\bar{m}\bar{n},y} g_{ymn}\,\mathrm{d}x\,\mathrm{d}y \tag{A7}$$

$$C_{2mn\bar{m}\bar{n}} = D_0 \int_0^{l_x}\int_0^{l_y} \left[-\nu (d g_{x\bar{m}\bar{n},x})_{,y} - \frac{1-\nu}{2} (d g_{x\bar{m}\bar{n},y})_{,x}\right] g_{ymn}\,\mathrm{d}x\,\mathrm{d}y \tag{A8}$$

$$C_{3mn\bar{m}\bar{n}} = \int_0^{l_x}\int_0^{l_y} [\kappa_0 G_0 h_0 \alpha_{Gy} g_{y\bar{m}\bar{n}} - D_0 (d g_{y\bar{m}\bar{n},y})_{,y} - \frac{1-\nu}{2} D_0 (d g_{y\bar{m}\bar{n},x})_{,x}] g_{ymn}\,\mathrm{d}x\,\mathrm{d}y \tag{A9}$$

and the terms of external loads are

$$P_{mn} = \int_0^{l_x}\int_0^{l_y} p f_{mn}\,\mathrm{d}x\,\mathrm{d}y \tag{A10}$$

They may be calculated easily by the method shown in Appendix 2.

APPENDIX 2. CALCULATION INCLUDING A SPECIFIC FUNCTION $D(x-x_i)$

The integral calculation including the specific function $D(x-x_i)$ can be written, from Takabatake (1991a), as

$$\int_0^{l_x} D(x-x_i) f(x)\,\mathrm{d}x = \int_{x_i-(b_{xi,j}/2)}^{x_i+(b_{xi,j}/2)} f(\xi)\,\mathrm{d}\xi \tag{A11}$$

in which ξ is a supplementary variable of x. The nth derivatives of the specific functions can therefore be expressed as

$$\int_0^{l_x} D^{(n)}(x-x_i) f(x)\,\mathrm{d}x = \int_{x_i-(b_{xi,j}/2)}^{x_i+(b_{xi,j}/2)} (-1)^n f^{(n)}(\xi)\,\mathrm{d}\xi \tag{A12}$$

in which the superscripts enclosed within parentheses indicate the differential order. For calculations including the specific function $D(y-y_j)$ similar expressions may be obtained.

When the conditions $b_{xi,j} \ll l_x$ and $b_{yi,j} \ll l_y$ are satisfied, the specific functions $D(x-x_i)$ and $D(y-y_j)$ are approximately related to the Dirac functions, $\delta(x-x_i)$ and $\delta(y-y_j)$, by:

$$D(x-x_i) \approx b_{xi,j}\delta(x-x_i)$$
$$D(y-y_j) \approx b_{yi,j}\delta(y-y_j). \tag{A13}$$